ACCOUNTS
of chemical research

Conformation and Energy Transfer in Single Conjugated Polymers

JOSHUA C. BOLINGER, MATTHEW C. TRAUB,
JOHANNA BRAZARD, TAKUJI ADACHI, PAUL F. BARBARA, AND
DAVID A. VANDEN BOUT*

RECEIVED ON JANUARY 10, 2012

CONSPECTUS

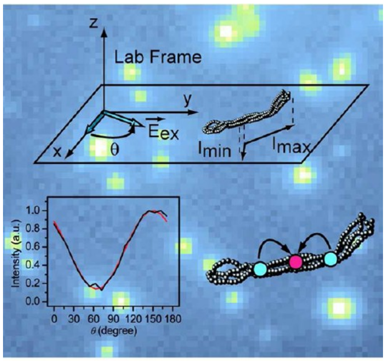

In contrast to the detailed understanding of inorganic materials, researchers lack a comprehensive view of how the properties of bulk organic materials arise from their individual components. For conjugated polymers to eventually serve as low cost semiconductor layers in electronic devices, researchers need to better understand their functionality. For organics, traditional materials science measurements tend to destroy the species of interest, especially at low concentrations. However, fluorescence continues to be a remarkably flexible, relatively noninvasive tool for probing the properties of individual molecules and allows researchers to carry out a broad range of experiments based on a relatively simple concept. In addition, the sensitivity of single-molecule spectroscopy allows researchers to see the properties of an individual component that would be masked in the bulk phase.

In this Account, we examine several photophysical properties of different conjugated polymers using single-molecule spectroscopy. In these experiments, we probed the relationship between the conformation of single conjugated polymer chains and the distance scale and efficiency of energy transfer within the polymer. Recent studies used polarization anisotropy measurements on single polymer chains to study chain folding following spin-casting from solution. This Account summarizes the effects of monomer regioregularity and backbone rigidity, by comparing a regiorandom phenylene vinylene (MEH-PPV) with both a regiorandom and regioregular thiophene (P3HT). Synthesis of novel polymers allowed us to explore the role of different conformation-directing inclusions in a PPV backbone. We showed that these inclusions control the conformation of individual chains and that molecular dynamics can predict these structural effects. *In situ* solvent vapor annealing studies explored the dynamics of polymer chains as well as the effect of solvent evaporation on the structural equilibrium of the polymer. We observed that a slower rate of solvent evaporation results in a narrow population of highly ordered polymer chains.

These highly ordered single chains serve as a model system to probe the effect of conformation on energy transfer following excitation in single MEH-PPV polymer chains in two distinct experiments. In the first, we correlated the anisotropy of the fluorescence emission of individual chains with the anisotropy of their fluorescence excitation. Using this data, we derived a model for energy transfer in a conjugated polymer, simulating chromophores along a chain, coupled via Förster energy transfer. In the second experiment, super-resolution measurements demonstrated the ability of single-molecule spectroscopy to directly visualize energy transfer along a polymer chain embedded in a model device environment. A capacitive device allowed for controlled localization of hole polarons onto the polymer chain. These positive charges subsequently quenched local excitations, providing insight into the range of energy transfer in these single polymer molecules.

As researchers continue to characterize conjugated polymer films and develop methods for creating multichain systems, single-molecule techniques will provide a greater understanding of how polymer morphology influences interchain interactions and will lead to a richer description of the electronic properties of bulk conjugated polymer films.

Introduction

Conjugated polymers (CPs) continue to attract interest as materials for use in organic electronic devices such as light emitting diodes,[1] chemical sensors,[2] solar cells,[3] and transistors.[4] The performance of the active layer in these devices, typically a thin film of neat CP or a polymer/small molecule blend, depends not only on the band energies of these films but on the film's energy and charge transport properties. While measurement of thin-film electronic properties is often straightforward, our understanding of how

10.1021/ar300012k

these properties arise from the interactions of individual chains is limited. Because of the complex heterogeneity of the films, their properties are often the ensemble sum of many different interactions. By studying single polymer chains, we can begin to uncover how chain conformation influences different properties.

Spectroscopists have generally treated CP chains as an interconnected system of fluorescent chromophores,[5−7] allowing quantitative simulations and descriptions of experimental results. Previous work has used this model to approach such varied topics as the nature of energy migration following photoexcitation,[8,9] the existence of low-energy "red" sites,[10,11] the effects of hole polarons on singlet excitons in a device-like environment,[12,13] and the conformations assumed by a single chain.[14−17] These studies lead to more detailed questions concerning the structure/function relationship of CP molecules.

This Account reviews single-molecule experiments on conjugated polymers focusing primarily on structure and its effects on energy transfer. The first part discusses the use of polarization excitation anisotropy to probe conformation of individual polymer chains, providing insight into the collapsed structures formed during spin-casting into an inert host matrix. Studies presented here compare two CP backbones, thiophenes (P3HT, regiorandom and regioregular) and phenylene vinylenes (MEH-PPV). Other work describes how chain folding is influenced by synthetic inclusions. Finally, the effects of solvent processing on single molecules were probed with studies on *in situ* solvent vapor annealing of CPs that results in a single population of highly aligned, folded chains. Together, the work in this section provides an extensive description of CP structure at the molecular level.

The second part of this Account describes how single-molecule structure can be used to quantitatively describe energy transfer in CPs. The first study discusses experiments where MEH-PPV polarization excitation anisotropy is correlated with emission anisotropy. This correlation study provides the framework for a model of energy transfer in a multichromophoric system. Second, building on previous work studying polaron-singlet exciton interactions of single CP chains in a device environment, subdiffraction localization techniques have been employed to measure the distance scale for energy transfer from excitons to trapped hole polarons. The observed quenching and large observed shifts in the centroid of the fluorescence point spread function demonstrate the existence of long-range energy transfer (>40 nm) in these structures and provide evidence for an elongated conformation with a length of at least 50 nm along the major axis.

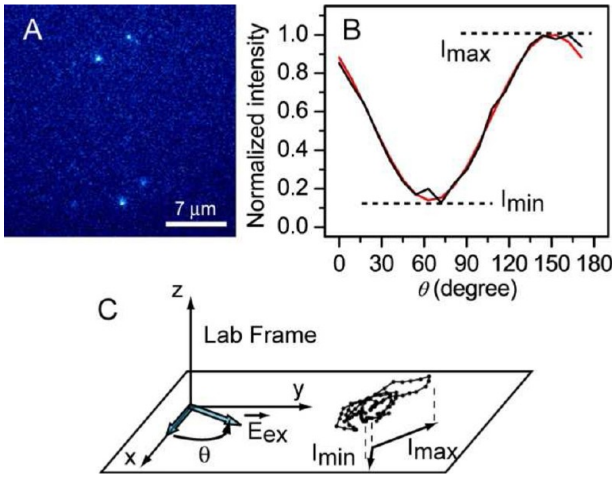

FIGURE 1. (A) Wide-field fluorescence microscope image of P3HT. (B) A representative fluorescence intensity trace as a function of excitation polarization angle, θ. The black line is experimental data and the red line is the fitted curve. (C) Schematic representation of the polarization excitation experiments. E_{ex} is the direction of linearly polarized excitation at time *t*. Adapted from ref 19.

Conjugated Polymer Structure at the Single Chain Level

Three prototypical CPs, regiorandom (*rra*-) MEH-PPV and regioregular (*rr*-) P3HT and *rra*-P3HT, were studied by single-molecule fluorescence excitation polarization spectroscopy to determine whether their macroscopic structural properties persist at the single-molecule level. The morphological order of single CP chains was evaluated by measuring the modulation depth, *M*, of highly diluted samples embedded in a PMMA matrix on a home-built wide-field microscope.[18] The total fluorescence intensity was collected while linearly polarized excitation was rotated in the $x-y$ plane of the sample (Figure 1C). A fluorescence image of single CP chains is shown in Figure 1A. The fluorescence intensity of each CP chain was fitted as a function of the excitation polarization angle, θ, as described in eq 1 where Φ is the angle of maximum absorption (Figure 1B).

$$I \propto 1 + M\cos 2(\theta - \Phi) \qquad (1)$$

The parameter *M* is the projection of the absorption tensor onto the $x-y$ plane of the laboratory frame. The absorption tensor for CP chains is the sum of all individual transition dipoles (i.e., chromophores) along the chain. The modulation depth ranges from 0 to 1, corresponding to totally isotropic and anisotropic conformations, respectively.

Previous work by Hu et al. found a broad range of conformations for single chains of *rra*-MEH-PPV.[14] With recent improvements in the synthesis and experimental apparatus, the polarization excitation experiments for

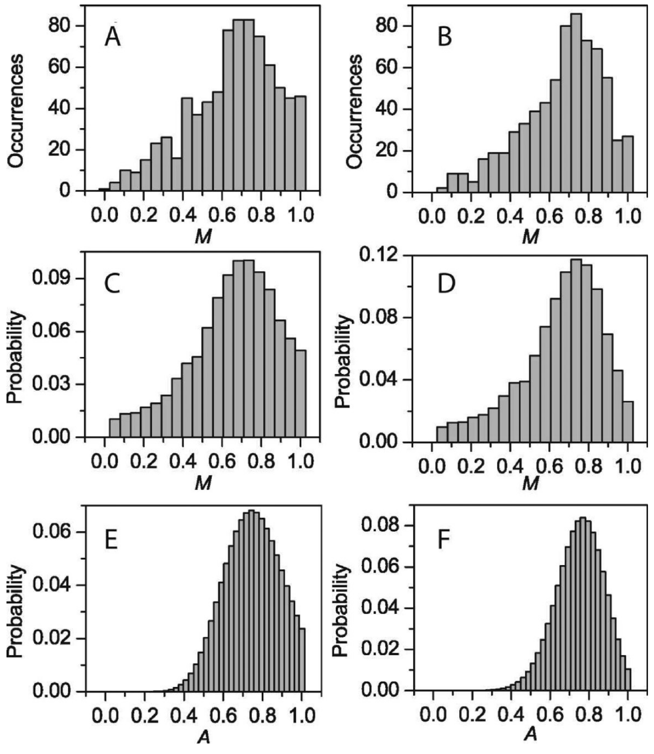

FIGURE 2. (A, B) The experimental histogram of modulation depth, *M*, from 798 150-kDa MEH-PPV molecules and 692 2600-kDa MEH-PPV molecules, respectively. (C, D) The best fit histograms for the data shown in panels A and B calculated by least-squares fitting procedures. (E, F) Anisotropy, *A*, distribution resolved by the best fit that generated the data shown in panels C and D. Adapted from ref 18.

single-molecule *rra*-MEH-PPV have been repeated.[18] These new studies suggest that the majority of the single chains fold into highly anisotropic conformations consistent with the rod structure put forth by Hu et al.[14] Histograms of the excitation modulation depth of *rra*-MEH-PPV (Figure 2A,B) show little difference with increasing molecular weight. After fitting these experimental modulation depth histograms to account for the out-of-plane tilt angle for each molecule and experimental artifacts introduced by the high numerical aperture objective, no anisotropy below 0.3 was observed in the real anisotropy histograms (Figure 2E,F), in good agreement with the rod-like structure. The experimental modulation depth histograms could be accurately simulated by coarse-grained beads-on-a-chain models only when a tetrahedral-defect was inserted in the middle of the CP chains, suggesting that the observed rod-like structures may be explained by the presence of thermally induced defects along the chains. Absent the tetrahedral defect in the chain, the beads-on-a-chain model could not reproduce anisotropies about 0.7.

Another question to address is the importance of the regioregularity on the morphology of CP chains.[19] While *rra*-MEH-PPV and *rra*-P3HT are known to generate amorphous films, single molecules of *rra*-MEH-PPV fold into highly ordered rod conformations. In contrast, *rra*-P3HT shows a much broader distribution of conformations, from highly ordered to highly disordered (Figure 3B,D), an effect that is not correlated to molecular weight.[19] In the case of *rr*-P3HT, bulk films are highly crystalline,[20] and single chains of rr-P3HT are highly ordered (Figure 3A,C) indicating that the regioregularity is more important in determining the morphology of P3HT than of MEH-PPV. This clearly demonstrates that coarse-grained beads-on-a-chain models that do not include explicit side chains will be insufficient for P3HT where conformations are strongly affected by side-chain interactions.

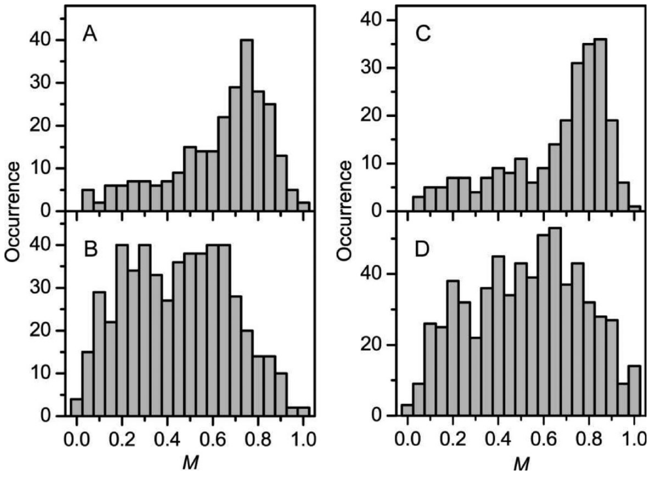

FIGURE 3. The experimental *M* histograms of (A) *rr*-P3HT ($M_n = 148$ kDa, PDI = 1.35, 97% HT-HT) from 262 molecules, (B) *rra*-P3HT ($M_n = 191$ kDa, PDI = 1.33, 64% HT-HT) from 526 molecules, (C) *rr*-P3HT ($M_n = 35$ kDa, PDI = 1.45) 242 molecules, and (D) *rra*-P3HT ($M_n = 45$ kDa, PDI = 1.10) 646 molecules. Adapted from ref 19.

Conformational Control of Conjugated Polymers through Synthetic Inclusions

Previous work done by Barbara et al. demonstrated the effect of tetrahedral defect inclusions on the conformation and energy transfer properties of CPs.[14,21] In recent work by Bounos et al., MEH-PPV copolymers were synthesized via the Horner method with morphology directing inclusions randomly inserted into the backbone.[22] Three types of inclusions were studied: a *para*-terphenyl group that preserves the highly linear nature of MEH-PPV, a highly bent, rigid *ortho*-terphenyl group that mimics the effects of cis-defects in the backbone and, at high concentrations, disrupts the single-molecule conformation of MEH-PPV, and a flexible "saturated" linker that mimics the effects of a tetrahedral defect, allowing for a high degree of rotational flexibility in

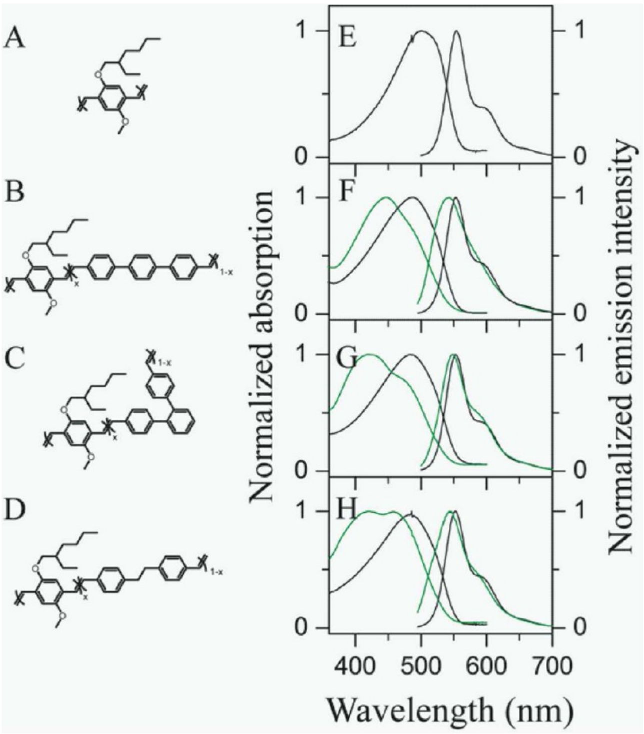

FIGURE 4. (A−D) Structures of MEH-PPV, *para*-terphenyl-MEH-PPV, *ortho*-terphenyl-MEH-PPV, and saturated MEH-PPV, respectively. (E−H) Absorption and emission spectra of the corresponding polymers are shown to the left. In panels F−H, 10% defect inclusion is shown in black and 30% defect inclusion shown in green. Adapted from ref 22.

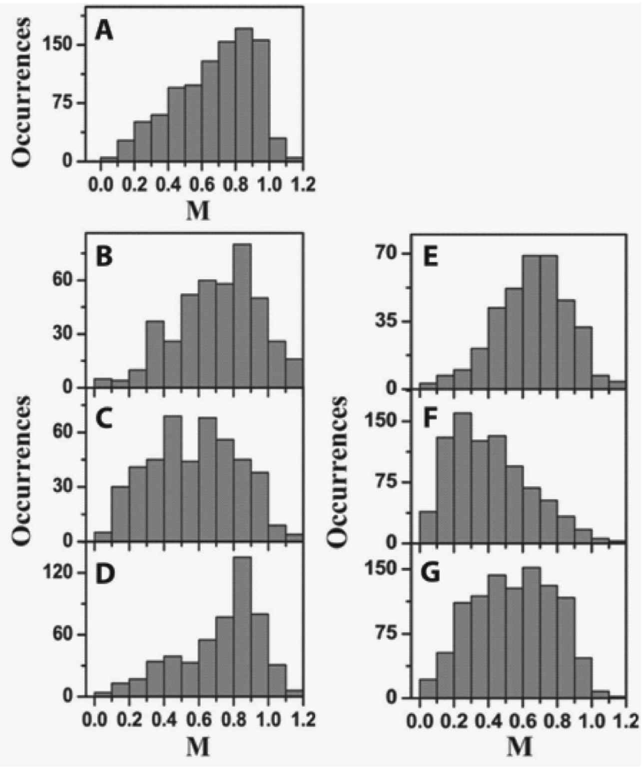

FIGURE 5. Experimental histograms of modulation depth, *M*, obtained with 488-nm excitation: (A) MEH-PPV (981 molecules), (B) 10% *para*-terphenyl-MEH-PPV (424 molecules), (C) 10% *ortho*-terphenyl-MEH-PPV (454 molecules), and (D) 10% saturated MEH-PPV (524 molecules). Experimental histograms of modulation depth, *M*, obtained with 457-nm excitation: (E) 30% *para*-terphenyl-MEH-PPV (362 molecules), (F) 30% *ortho*-terphenyl-MEH-PPV (862 molecules), and (G) 30% saturated MEH-PPV (1033 molecules). Adapted from ref 22.

the chain. These inclusions sever the conjugation in the CP backbone and shorten the average effective chromophore length, as demonstrated by the solution-phase absorption and fluorescence spectra (Figure 4E−H). Recent lifetime measurements on the "defected" PPVs demonstrate a shortened fluorescence lifetime, consistent with the smaller oscillator strength of shorter oligomers.[23] While the absorption shifts dramatically to higher energy with increasing defect concentration, the fluorescence only shows modest hypsochromic shifts. Due to the random nature of the defect inclusion, there still exist a finite number of longer, lower energy chromophores to which energy funnels, limiting the effect of chromophore shortening on the emission spectra.

The modulation depths for single chain excitation polarization on the inclusion polymers, as well as pristine MEH-PPV, are presented in Figure 5. Figure 5A is the histogram for MEH-PPV (mean = 0.67) while Figure 5B−H shows the different 10% and 30% inclusion species. The linear *para*-terphenyl-MEH-PPV results are presented in Figure 5B,F. The *para*-terphenyl inclusion maintained the rod-like structure of pristine MEH-PPV, and both 10% and 30% demonstrate a similar distribution of modulation depths with average values of 0.67 and 0.64, respectively, preserving MEH-PPV's native collapsed conformation.

The modulation depths for 10% and 30% *ortho*-terphenyl-MEH-PPV are presented in Figure 5C,G, respectively. The 10% *ortho*-terphenyl-MEH-PPV polymer chains demonstrate a flat distribution of modulation depths between 0.1 and 1, suggesting that at this inclusion level, the polymer chains are capable of assuming a wide variety of conformations. At 30% inclusion, the histogram is broadly peaked at 0.3 with highly anisotropic polymer chains only comprising the tail of the distribution. While the lowering of the modulation depth due to the disruptive presence of the forced kink was anticipated, the persistence of chains with high modulation depths for the highly defected species, even in small quantities, was surprising. Molecular dynamics (MD) simulations from this work demonstrate that the position of the inclusion species along the polymer backbone strongly influences the folding of the chain leading to either a highly ordered, anisotropic structure or a disordered, more isotropic structure.

The modulation depth histograms for 10% and 30% saturated inclusion MEH-PPV are presented in Figure 5D,H, respectively. At 10% inclusion, the distribution of modulation depths is peaked at 0.85, similar to MEH-PPV; however the distribution is much sharper. From the MD simulations and the solvent vapor annealing work discussed below, it appears that the folding of the chain during the spin-casting process is sensitive to the rapid change in chain environment from solvent to host matrix. The narrow distribution observed in this study is perhaps indicative of the relative ease of chain folding due to the rotational freedom afforded by the saturated linker. At 30% inclusion, similar to 10% *ortho*-terphenyl-MEH-PPV, the saturated linker produces a very broad histogram of modulation depths with a nearly static probability from 0.2 to 0.9. At this high level of inclusion, it is equally probable that a chain will fold into either high or low anisotropy molecules. This is likely due to the random nature of inclusion incorporation, where the flexibility of each individual chain depends on the number and position of the inclusions incorporated into the backbone.

Solvent Vapor Annealing of Single Polymer Chains

Solvent vapor annealing (SVA) is a processing technique that improves functionality, reliability, and performance in polymer devices.[24] Vogelsang et al. introduced a new technique to monitor single polymer chains during solvent vapor annealing.[25] A home-built flow cell coupled with a fluorescence microscope allows for the inspection of single polymer chains of MEH-PPV before, during, and after introducing a solvent vapor that induces SVA of both the PMMA matrix and the MEH-PPV single chains.

Figure 6 shows wide-field images of single chains of MEH-PPV in a PMMA film before, during, and after SVA as well as fluorescence correlation spectroscopy (FCS) measurements for these different states. Before and after SVA, individual molecules are clearly visible in the wide-field image, while FCS data on individual molecules indicate no movement. During SVA, molecules appear elongated in the wide-field images due to translational diffusion. FCS revealed a broad range of time scales of motion ranging from molecules that are stationary on the second scale to molecules that diffuse in a liquid-like state on the millisecond scale. The glass transition temperature depends on the concentration of toluene that has penetrated into the film, allowing for the distribution of time scales associated with the movement of MEH-PPV in the PMMA film during SVA observed with FCS. The Vacha group has recently tracked single molecules for seconds in liquid environments utilizing concentrated solutions of polystyrene in toluene, demonstrating similar results with more uniform diffusion speeds.[26]

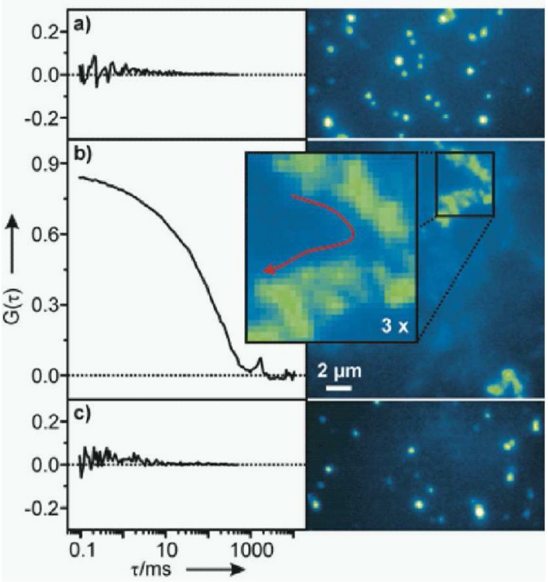

FIGURE 6. Fluorescence correlation spectroscopy (FCS) and wide-field fluorescence images of MEH-PPV/PMMA thin films under different processing conditions. The FCS curves on the left are acquired from a PMMA film with an average concentration of MEH-PPV of ~1 molecule/μm^2 before (a), during (b) and after (c) SVA. On the right, wide-field fluorescence images are shown of a PMMA film containing MEH-PPV molecules before (a), during (b) and after SVA (c). The red arrow corresponds to a molecule that undergoes translation. The images are averaged over 180 images with an integration time of 1 s each. Adapted from ref 25.

Polarization excitation fluorescence was used to investigate the structure of the CP chains before and after SVA. Figure 7A shows the modulation depth of MEH-PPV single chains in PMMA spun from toluene while Figure 7B shows those from chloroform. Histograms of chloroform-spun MEH-PPV contain a population of molecules with low modulation depths, an observation attributed to the lower boiling point of chloroform compared with toluene. In solution, chains of MEH-PPV most likely adopt elongated conformations. Upon evaporation of the solvent, the concentration of PMMA, a poor “solvent” for MEH-PPV, increases inducing the MEH-PPV to collapse on itself. The rapid rate of solvent evaporation in the chloroform case affords the MEH-PPV chains less time to organize, resulting in a subpopulation of chains frozen in a partially collapsed state. Following SVA with toluene, modulation depth histograms for both samples are nearly identical as shown in Figure 7C,D. The subpopulation of low modulation depth molecules found in chloroform disappears, resulting in a single, narrow population distribution of highly anisotropic molecules (see Figure 7F). While the toluene spun

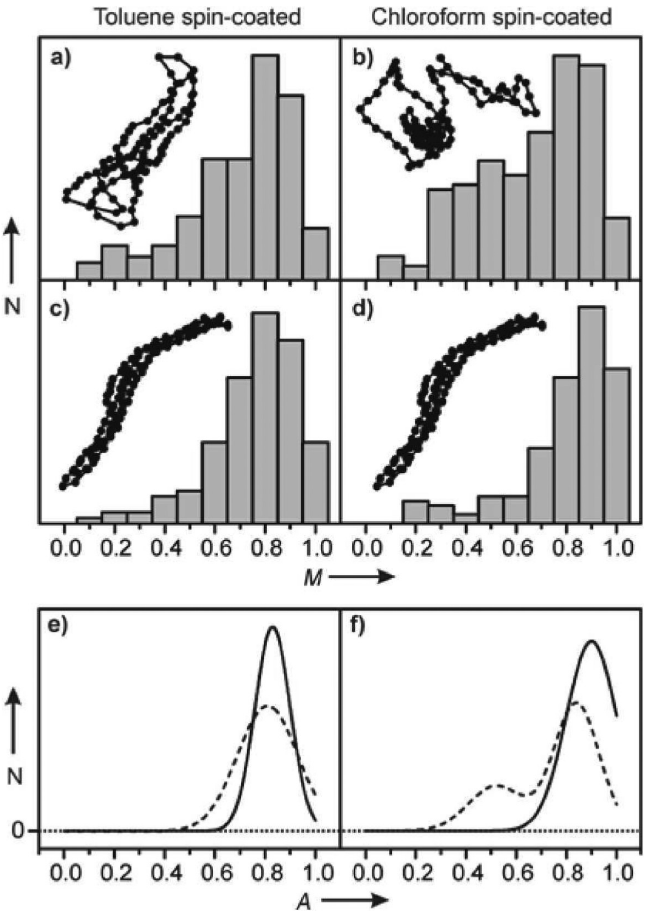

FIGURE 7. The experimental histograms of modulation depth, *M*, from single MEH-PPV molecules ($M_W = 830$ kDa) in a PMMA host matrix with different preparation methods: Spin-coated from (a) toluene and (b) chloroform solution. The samples were additionally solvent vapor annealed for 60 min (c, d). The histograms consist of 152, 230, 160, and 146 MEH-PPV molecules for panels a, b, c, and d, respectively. The insets illustrate a conformation of the molecule consistent with the histogram average. (e, f) Anisotropy, *A*, distributions before (striped lines) and after SVA (solid lines) fit from panels a–d. Adapted from ref 25.

sample originally showed little evidence of a subpopulation of low modulation depth molecules, the distribution of modulation depths was broader before SVA (see Figure 7E), demonstrating that while MEH-PPV spun from toluene is mostly folded into a rod-like structure, there is still some heterogeneity in chain conformations from the as-spun sample. The SVA annealing work suggests that for MEH-PPV single chains embedded in PMMA, there exists a single, highly ordered conformation and SVA allows the chains to overcome the kinetic barrier imparted by the spin-casting process.

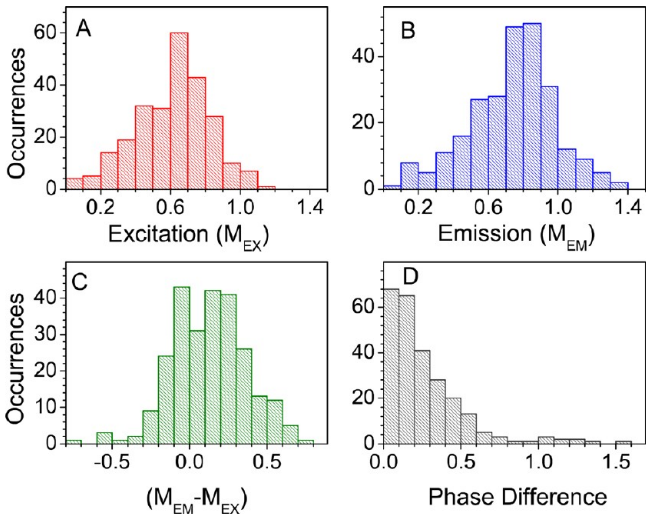

FIGURE 8. Histogram of modulation depths for (A) excitation and (B) emission for 150 kDa MEH-PPV single molecules. (C) Change in anisotropy from excitation to emission for each molecule. (D) phase angle difference between excitation and emission. Adapted from ref 27.

Understanding Energy Transfer Through Structure

The uniformity of conformation and high degree of order observed in MEH-PPV single molecules provides a unique environment to probe the effects of structure on energy transfer in CPs. Alignment of chromophores within each chain facilitates efficient long-range energy funneling of excited states to low energy sites. Traub et al. probed this relationship between structure and energy transfer by simultaneously measuring the excitation and emission polarization anisotropy of single MEH-PPV chains.[27] Previous studies from other groups have demonstrated the utility of this technique for studying energy transfer in CP systems.[9,28−30] Polarized excitation democratically excites the chromophores and yields a modulation depth (M_{ex}) corresponding to the overall shape of each chain. Energy transfer from high-energy to low-energy chromophores results in a majority of the emission occurring from a subset of the chromophores. Polarized detection provides an emission modulation depth (M_{em}) corresponding to the alignment of the sites responsible for emission.

Statistical treatment of these observables over many molecules allowed a qualitative description of energy transfer in aligned MEH-PPV chains (Figure 8). Electronic energy transfer to selected sites is known to yield increases in modulation depth.[29] The small average change in the in-plane dipole orientation (<15°) is consistent with chromophores whose alignment is already nearly uniform, where energy transfer to any given subset of chromophores does not yield a substantial change in average dipole orientation. However, a more quantitative description of these results requires explicit consideration of polymer conformation.

Monte Carlo simulated polymer chains were used to simulate the experimentally observed histograms. For a

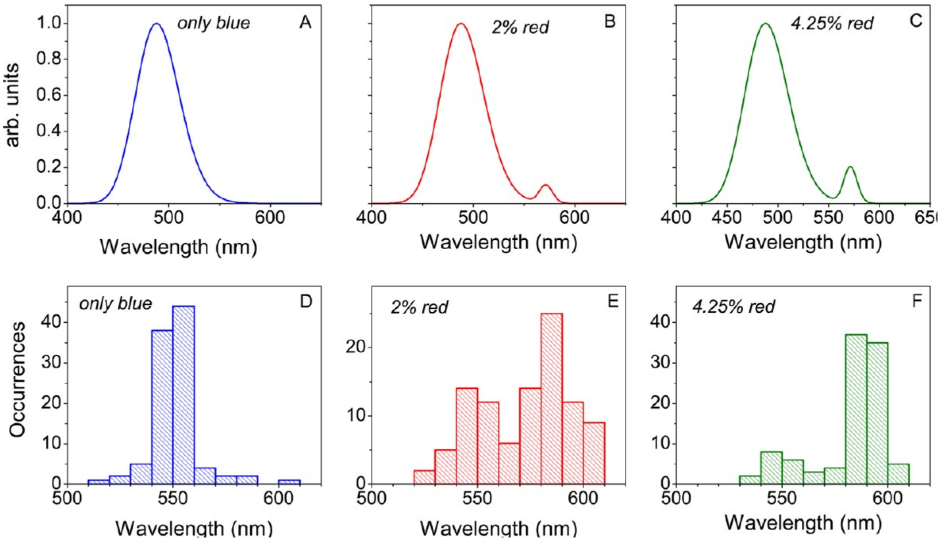

FIGURE 9. The bigaussian energy distribution (with peak wavelengths 488 nm [blue] and 570 nm [red]) inputs given to model 150 kDa MEH-PPV single chains for FRET simulations with (A) only blue sites, (B) 2% red sites, and (C) 4.25% red sites. Panels D–F are the respective histograms for peak position of single-molecule emission energies obtained from the FRET simulations. Adapted from ref 27.

series of bead-on-a-chain model conformations, energies were randomly assigned to chromophore sites from an energy distribution derived from the MEH-PPV solution absorption spectrum. By accounting for spectral overlap with the excitation, and the out of plane tilt, these initial energy distributions generated simulated excitation modulation depths for the model chains. Energy transfer was then allowed to proceed via a Förster (point dipole) mechanism, based on chain conformation and spectral overlap between the chromophores in each distribution. The highly aligned model chains facilitated efficient energy transfer, and the majority of the emission occurred typically from 5 to 10 chromophores out of the 200 total chromophores in each chain.

This energy transfer model was also used to simulate emission peaks of single MEH-PPV molecules, which are bimodally distributed between "blue" ($\lambda \approx 550$ nm) and "red" ($\lambda \approx 585$ nm) values. The single-molecule ensemble emission peak histogram was best reproduced by using a probability distribution in which each chromophore had a 2–3% probability of being a red site (Figure 9). Increasing the number of red sites per chain resulted in emission almost exclusively from red sites, a clear demonstration of how organized structures can facilitate efficient capture of excitons by low-energy traps in CP. It should be noted that the effective chromophore size in our model chains was too small to apply line dipole approximations that more accurately describe energy transfer in these systems. Thus, these simulations represent a lower limit for energy transfer in MEH-PPV and a potential starting point for future quantitative descriptions of these systems.[31,32]

Visualizing Exciton to Polaron Energy Transfer in Single Polymer Chains

Previous work on single-molecule hole injection by the Barbara lab demonstrated reproducible charge injection into single chains of MEH-PPV in a capacitor type hole-only device (Figure 10A).[12,13] These devices provided a way to controllably and reversibly inject charge by changing the bias on the device. Bolinger et al. used fluorescence quenching by hole polarons for the study of charge trapping and energy transfer in single molecules.[33]

The study of these devices demonstrated strong photostability for single-molecule fluorescence studies. The ability of a single chain to emit a high number of photons under these conditions makes it ideal for point spread fitting (Figure 10B).[34] Point spread function (PSF) fitting of single dye molecules provides centroid accuracy on the order of 10–20 nm and has been used to estimate the size of CPs based on centroid shifts during photooxidation,[35] but with the enhanced stability of single chains in the device environment, the accuracy that can be achieved with PSF is on the order of a few angstroms. With the hole-injection devices as discussed above, sufficient bias is applied to quench the single chains by ~50% (see Figure 10C). This statistically corresponds to the quenching depth of a single hole for a chain of MEH-PPV.[36] By fitting the PSF of the single chains before and after charge injection, we can obtain information about the size of the chains and the range of energy transfer within them.

Hole polarons trapped on the chain locally quench excitations on neighboring chromophores, while energy transfer

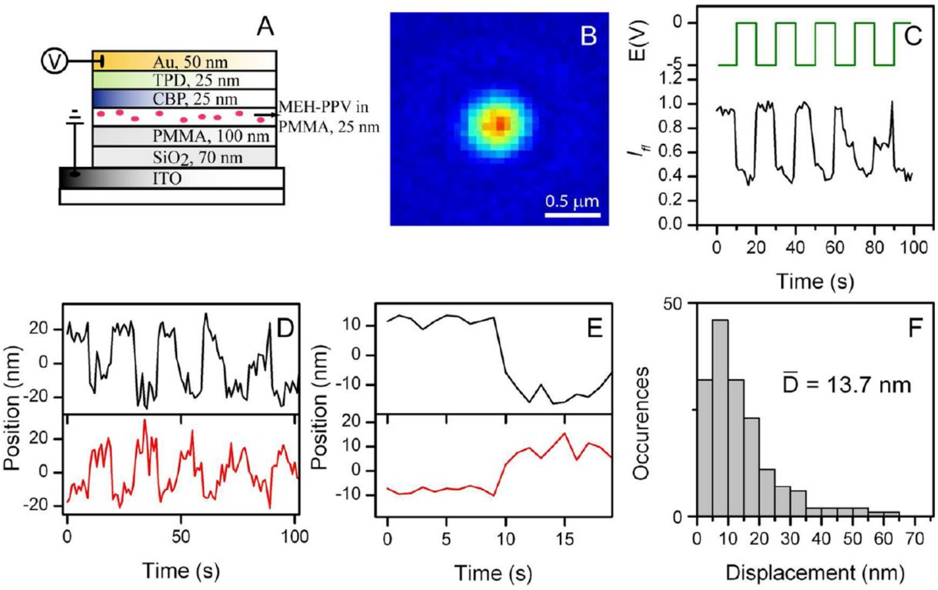

FIGURE 10. (A) Structure of the hole injection device used in these studies. (B) False color image of a single molecule of MEH-PPV in the device. (C) $F-V$ measurement of the molecule shown in panel B with fluorescence transient in black and the applied bias in green. (D) The centroid displacement of the point spread function resulting from the applied bias shown in panel C where displacement in the x (black) and y (red) direction is shown. (E) Synchronized average of the X (black line) and Y (red line) centroid displacement obtained from panel D. (F) Histogram of the total centroid displacement ($D = (X^2 + Y^2)^{1/2}$) for 167 single-molecule MEH-PPV (MW = 150 kDa) transients. Values peak at 9.8 nm with a mean of 13.7 nm. Adapted from ref 33.

within the chain to sites near the polaron increases its effective quenching radius. Figure 10D demonstrates the observed shift in the centroid position of the fluorescence PSF of an individual molecule in the x- and y-axes of the CCD detector in the presence of a hole polaron quenching the fluorescence intensity by half. The centroid position shifts are repeatable from bias cycle to bias cycle, implying that the location on the polymer chain for hole trapping is identical. Figure 10E shows the x- and y-centroid position synchronously averaged over multiple bias cycles. Figure 11F is a histogram of centroid displacements for individual molecules after fluorescence quenching of 40−60%. The average centroid displacement observed for MEH-PPV is 13.7 nm. However, a population of molecules demonstrates displacements of 30 nm or greater. Modeling of the displacement reveals that the displacement values are on average only ∼1/3 of the energy transfer distances. Thus large displacements of 30 nm would correspond to energy transfer distances of 75 nm, a value that is substantially larger than the bulk exciton migration value for MEH-PPV (∼5−10 nm).

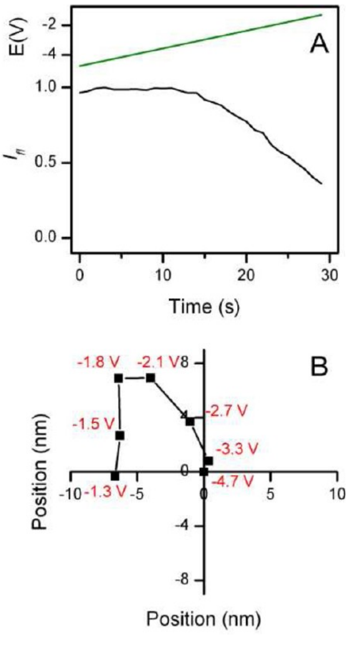

FIGURE 11. (A) Fluorescence transient of a single molecule (black) with the bias applied as shown above (green). (B) Centroid position obtained from the single molecule shown in panel A with the voltage for each point shown in red (points omitted for clarity). Adapted from ref 33.

The application of a sawtooth bias allows for fractional injection of hole polarons into a polymer chain. Figure 11A shows the applied bias and fluorescence intensity verses time for a single polymer chain. Figure 11B plots the centroid position as a function of device bias. Starting at −3.3 V, the centroid position moves linearly with increasing bias. At −2.1 V, the centroid position shift changes directions, and at −1.8 V, it shifts directions again. These changes in direction are attributed to multiple hole injection, with each sequential hole becoming trapped at different locations on the polymer chain. This study presents evidence that hole trapping in this system does not occur via bipolaron formation but that holes migrate to low-energy sites within the polymer chain where the position of these hole traps is likely dictated by polymer conformation.

Conclusion

The study of conjugated polymers at the single-molecule level revealed a strong relationship between structure and energy transfer along the chain. Polarization modulation studies of single molecules of both MEH-PPV and P3HT show that conformation of individual chains depends on the defects in the polymer as well as the polymer side chains. From these studies, it is found that high molecular weight samples of MEH-PPV nearly all fold into anisotropic conformations that are very close to their equilibrium conformations. Individual polymer molecules allow for the detection of energy transfer along the backbone by both correlated excitation emission polarization modulation and centroid displacement imaging. Energy transfer reveals that the exciton diffusion length in these highly ordered conjugated polymers occurs on substantially longer distance scales than has been observed in bulk film. These single-molecule studies lay the foundation for work that bridges the gap between single chains and bulk films by examining small assemblies of individual chains.[23,37] Using studies of single molecules and single aggregates, we can build up a complete picture of how morphology and properties of conjugated polymer films evolve from individual chains up to bulk films.

Financial support was provided by the Welch Foundation and the U.S. Department of Energy (DOE-BES), as part of the program "Understanding Charge Separation and Transfer at Interfaces in Energy Materials (EFRC:CST)", an Energy Frontier Research Center funded under Award Number DE-SC0001091 as well as DE-FG02-ER15746. Additional support was provided as part of the program "Molecular Tools for Conjugated Polymer Analysis and Optimization", a Center for Chemical Innovation under NSF Award No. CHE-0943957. The authors also thank our numerous co-workers that are listed in many of the references of this paper.

BIOGRAPHICAL INFORMATION

Joshua C. Bolinger obtained his Ph.D. in 2006 in the group of Prof. Phillip Reid at the University of Washington, Seattle, where he worked on solution phase ultrafast spectroscopy. He then did postdoctoral research in the group of Prof. Paul Barbara at the University of Texas, where he studied the photophysics of conjugated polymers.

Matthew Traub obtained his Ph.D. at the California Institute of Technology for work with Professor Nathan Lewis on chemical functionalization and electronic passivation of semiconductor surfaces. After postdoctoral research with Professor Thomas Meyer at the University of North Carolina, Chapel Hill, he joined the group of Professor Paul Barbara at the University of Texas, studying structure and energy transfer in conjugated polymers. He has continued this work with Professor David Vanden Bout since Professor Barbara's death in 2010.

Johanna Brazard received her Ph.D. from Université Pierre et Marie Curie, France, in 2009 for work with Dr. Pascal Plaza at École Normale Supérieure on ultrafast photoprocesses in biological photoreceptors. Since she joined the group of Professor Paul Barbara at the University of Texas as a postdoctoral fellow, her work has focused on structure–function relationships in conjugated polymers by single-molecule spectroscopy. After Professor Paul Barbara's death in 2010, she has continued this work with Professor David Vanden Bout.

Takuji Adachi received his B.E. in 2006 in the group of Prof. Hiroshi Masuhara at Osaka University. He joined Prof. Paul Barbara's group in 2007 as a graduate student and has been involved in single-molecule spectroscopy of conjugated polymers.

Paul F. Barbara (1953–2010) received his Ph.D. in Chemistry in 1978 from Brown University working under R. G. Lawler. After his Ph.D. he carried out postdoctoral work at Bell Laboratories until he joined the faculty of the University of Minnesota in 1980. He achieved the rank of full professor in 1990 and in 1995 was named 3M-Alumni Distinguished Professor of Chemistry. In 1998, he moved to the University of Texas to fill the Richard J. V. Johnson Welch Chair in Chemistry, which he held along with the title Director of the Center for Nano- and Molecular Science and Technology until the time of his passing. He was a Senior Editor of *Accounts of Chemical Research* and a Past Chair of the Division of Physical Chemistry of the American Chemical Society. He was elected to the American Academy of Arts and Sciences in 1999 and was elected Fellow of the American Physical Society in 1993 and Fellow of the American Association for Advancement of Science in 2004. He was inducted into the United States National Academy of Science in 2006.

David A. Vanden Bout received his Ph.D. in 1995 from the University of Texas at Austin in ultrafast vibrational spectroscopy under the supervision of Dr. Mark Berg. After this he was a postdoctoral research fellow at the University of Minnesota with Dr. Paul Barbara before starting as an Assistant Professor in the Department of Chemistry & Biochemistry at the University of Texas at Austin in 1997. He was promoted to Associate Professor in 2001 and upon the death of Dr. Barbara took over supervision of his research group.

FOOTNOTES

The authors declare no competing financial interest.

REFERENCES

1 Friend, R. H.; Gymer, R. W.; Holmes, A. B.; Burroughes, J. H.; Marks, R. N.; Taliani, C.; Bradley, D. D. C.; Dos Santos, D. A.; Bredas, J. L.; Logdlund, M.; Salaneck, W. R. Electroluminescence in conjugated polymers. *Nature* **1999**, *397* (6715), 121–128.

2 McQuade, D. T.; Pullen, A. E.; Swager, T. M. Conjugated polymer-based chemical sensors. *Chem. Rev.* **2000**, *100* (7), 2537–2574.

3 Coakley, K. M.; McGehee, M. D. Conjugated polymer photovoltaic cells. *Chem. Mater.* **2004**, *16* (23), 4533–4542.

4 Facchetti, A. π-Conjugated polymers for organic electronics and photovoltaic cell applications. *Chem. Mater.* **2011**, *23* (3), 733–758.

5 Bassler, H.; Schweitzer, B. Site-selective fluorescence spectroscopy of conjugated polymers and oligomers. *Acc. Chem. Res.* **1999**, *32* (2), 173–182.

6 Lupton, J. M. Single-molecule spectroscopy for plastic electronics: Materials analysis from the bottom-up. *Adv. Mater.* **2010**, *22* (15), 1689–1721.

7 Barbara, P. F.; Gesquiere, A. J.; Park, S.-J.; Lee, Y. J. Single-molecule spectroscopy of conjugated polymers. *Acc. Chem. Res.* **2005**, *38* (7), 602–610.

8 Kim, D. Y.; Grey, J. K.; Barbara, P. F. A detailed single molecule spectroscopy study of the vibronic states and energy transfer pathways of the conjugated polymer MEH-PPV. *Synth. Met.* **2006**, *156* (2−4), 336–345.

9 Lin, H.; Tabaei, S. R.; Thomsson, D.; Mirzov, O.; Larsson, P.-O.; Scheblykin, I. G. Fluorescence blinking, exciton dynamics, and energy transfer domains in single conjugated polymer chains. *J. Am. Chem. Soc.* **2008**, *130* (22), 7042–7051.

10 Grey, J. K.; Kim, D. Y.; Norris, B. C.; Miller, W. L.; Barbara, P. F. Size-dependent spectroscopic properties of conjugated polymer nanoparticles. *J. Phys. Chem. B* **2006**, *110* (51), 25568–25572.

11 Feist, F. A.; Zickler, M. F.; Basché, T. Origin of the red sites and energy transfer rates in single MEH-PPV chains at low temperature. *ChemPhysChem* **2011**, 1499–1508.

12 Bolinger, J. C.; Fradkin, L.; Lee, K. J.; Palacios, R. E.; Barbara, P. F. Light-assisted deep-trapping of holes in conjugated polymers. *Proc. Natl. Acad. Sci. U.S.A.* **2009**, *106* (5), 1342–1346.

13 Bolinger, J.; Lee, K. J.; Palacios, R. E.; Barbara, P. F. Detailed investigation of light induced charge injection into a single conjugated polymer chain. *J. Phys. Chem. C* **2008**, *112* (47), 18608–18615.

14 Hu, D. H.; Yu, J.; Wong, K.; Bagchi, B.; Rossky, P. J.; Barbara, P. F. Collapse of stiff conjugated polymers with chemical defects into ordered, cylindrical conformations. *Nature* **2000**, *405* (6790), 1030–1033.

15 Ebihara, Y.; Vacha, M. A method for determining the absorption ellipsoid of single conjugated polymer molecules and single luminescent nanoparticles. *J. Chem. Phys.* **2005**, *123* (24), No. 244710.

16 Sartori, S. S.; De Feyter, S.; Hofkens, J.; Van der Auweraer, M.; De Schryver, F.; Brunner, K.; Hofstraat, J. W. Host matrix dependence on the photophysical properties of individual conjugated polymer chains. *Macromolecules* **2003**, *36* (2), 500–507.

17 Sun, W.-Y.; Yang, S.-C.; White, J. D.; Hsu, J.-H.; Pern, G. Y.; Chen, S. A.; Fann, W. Conformation and energy transfer in a single luminescent conjugated polymer. *Macromolecules* **2005**, *38* (7), 2966–2973.

18 Adachi, T.; Brazard, J.; Chokshi, P.; Bolinger, J. C.; Ganesan, V.; Barbara, P. F. Highly ordered single conjugated polymer chain rod morphologies. *J. Phys. Chem. C* **2010**, *114* (48), 20896–20902.

19 Adachi, T.; Brazard, J.; Ono, R. J.; Hanson, B.; Traub, M. C.; Wu, Z.-Q.; Li, Z.; Bolinger, J. C.; Ganesan, V.; Bielawski, C. W.; Bout, D. A. V.; Barbara, P. F. Regioregularity and single polythiophene chain conformation. *J. Phys. Chem. Lett.* **2011**, *2* (12), 1400–1404.

20 Kim, Y.; Cook, S.; Tuladhar, S. M.; Choulis, S. A.; Nelson, J.; Durrant, J. R.; Bradley, D. D. C.; Giles, M.; Mcculloch, I.; Ha, C. S.; Ree, M. A strong regioregularity effect in self-organizing conjugated polymer films and high-efficiency polythiophene: fullerene solar cells. *Nat. Mater.* **2006**, *5* (3), 197–203.

21 Wong, K. F.; Skaf, M. S.; Yang, C. Y.; Rossky, P. J.; Bagchi, B.; Hu, D. H.; Yu, J.; Barbara, P. F. Structural and electronic characterization of chemical and conformational defects in conjugated polymers. *J. Phys. Chem. B* **2001**, *105* (26), 6103–6107.

22 Bounos, G.; Ghosh, S.; Lee, A. K.; Plunkett, K. N.; DuBay, K. H.; Bolinger, J. C.; Zhang, R.; Friesner, R. A.; Nuckolls, C.; Reichman, D. R.; Barbara, P. F. Controlling chain conformation in conjugated polymers using defect inclusion strategies. *J. Am. Chem. Soc.* **2011**, *133* (26), 10155–10160.

23 Traub, M. C.; Vogelsang, J.; Plunkett, K. N.; Nuckolls, C.; Vanden Bout, D. A. Unmasking bulk exciton traps and interchain electronic interactions with single conjugated polymer aggregates. *ACS Nano* **2012**, *6* (1), 523–529.

24 Miller, S.; Fanchini, G.; Lin, Y. Y.; Li, C.; Chen, C. W.; Su, W. F.; Chhowalla, M. Investigation of nanoscale morphological changes in organic photovoltaics during solvent vapor annealing. *J. Mater. Chem.* **2008**, *18* (3), 306–312.

25 Vogelsang, J.; Brazard, J.; Adachi, T.; Bolinger, J. C.; Barbara, P. F. Watching the annealing process one polymer chain at a time. *Angew. Chem. Int. Ed.* **2011**, *50* (10), 2257–2261.

26 Onda, S.; Kobayashi, H.; Hatano, T.; Furumaki, S.; Habuchi, S.; Vacha, M. Complete suppression of blinking and reduced photobleaching in single MEH-PPV chains in solution. *J. Phys. Chem. Lett.* **2011**, *2* (21), 2827–2831.

27 Traub, M. C.; Lakhwani, G.; Bolinger, J. C.; Bout, D. V.; Barbara, P. F. Electronic energy transfer in highly aligned MEH-PPV single chains. *J. Phys. Chem. B* **2011**, *115* (22), 9941–9947.

28 Muller, J. G.; Lupton, J. M.; Feldmann, J.; Lemmer, U.; Scherf, U. Ultrafast intramolecular energy transfer in single conjugated polymer chains probed by polarized single chromophore spectroscopy. *Appl. Phys. Lett.* **2004**, *84* (7), 1183–1185.

29 Becker, K.; Lupton, J. M. Efficient light harvesting in dye-endcapped conjugated polymers probed by single molecule spectroscopy. *J. Am. Chem. Soc.* **2006**, *128* (19), 6468–6479.

30 Mirzov, O.; Bloem, R.; Hania, P. R.; Thomsson, D.; Lin, H. Z.; Scheblykin, I. G. Polarization portraits of single multichromophoric systems: Visualizing conformation and energy transfer. *Small* **2009**, *5* (16), 1877–1888.

31 Dykstra, T. E.; Hennebicq, E.; Beljonne, D.; Gierschner, J.; Claudio, G.; Bittner, E. R.; Knoester, J.; Scholes, G. D. Conformational disorder and ultrafast exciton relaxation in PPV-family conjugated polymers. *J. Phys. Chem. B* **2009**, *113* (3), 656–667.

32 Westenhoff, S.; Daniel, C.; Friend, R. H.; Silva, C.; Sundström, V.; Yartsev, A. Exciton migration in a polythiophene: Probing the spatial and energy domain by line-dipole Förster-type energy transfer. *J. Chem. Phys.* **2005**, *122* (9), No. 094903.

33 Bolinger, J. C.; Traub, M. C.; Adachi, T.; Barbara, P. F. Ultralong-range polaron-induced quenching of excitons in isolated conjugated polymers. *Science* **2011**, *331* (6017), 565–567.

34 Thompson, R. E.; Larson, D. R.; Webb, W. W. Precise nanometer localization analysis for individual fluorescent probes. *Biophys. J.* **2002**, *82* (5), 2775–2783.

35 Habuchi, S.; Onda, S.; Vacha, M. Mapping the emitting sites within a single conjugated polymer molecule. *Chem. Commun.* **2009**, *32*, 4868–4870.

36 Gesquiere, A. J.; Park, S.-J.; Barbara, P. F. Hole-induced quenching of triplet and singlet excitons in conjugated polymers. *J. Am. Chem. Soc.* **2005**, *127* (26), 9556–9560.

37 Vogelsang, J.; Adachi, T.; Brazard, J.; Bout, D. V.; Barbara, P. F. Self-assembly of highly ordered conjugated polymer aggregates with long-range energy transfer. *Nat. Mater.* **2011**, *10*, 942–946.